

Communication: Anion-specific response of mesoscopic organization in ionic liquids upon pressurization

Cite as: J. Chem. Phys. **148**, 211102 (2018); <https://doi.org/10.1063/1.5036588>

Submitted: 17 April 2018 . Accepted: 23 May 2018 . Published Online: 07 June 2018

 Fabrizio Lo Celso,  Alessandro Triolo,  Lorenzo Gontrani, and Olga Russina



View Online



Export Citation



CrossMark

ARTICLES YOU MAY BE INTERESTED IN

[Preface: Special Topic on Chemical Physics of Ionic Liquids](#)

The Journal of Chemical Physics **148**, 193501 (2018); <https://doi.org/10.1063/1.5039492>

[Communication: Investigation of ion aggregation in ionic liquids and their solutions with lithium salt under high pressure](#)

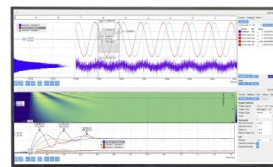
The Journal of Chemical Physics **148**, 031102 (2018); <https://doi.org/10.1063/1.5016049>

[Nanoscale organization in the fluorinated room temperature ionic liquid: Tetraethyl ammonium \(trifluoromethanesulfonyl\)\(nonafluorobutylsulfonyl\)imide](#)

The Journal of Chemical Physics **148**, 193816 (2018); <https://doi.org/10.1063/1.5016236>

Challenge us.

What are your needs for
periodic signal detection?



Zurich
Instruments

Communication: Anion-specific response of mesoscopic organization in ionic liquids upon pressurization

Fabrizio Lo Celso,^{1,2} Alessandro Triolo,² Lorenzo Gontrani,³ and Olga Russina^{3,a)}

¹*Dipartimento di Fisica e Chimica, Università di Palermo, Palermo, Italy*

²*Laboratorio Liquidi Ionici, Istituto Struttura della Materia, CNR (ISM-CNR), Rome, Italy*

³*Dipartimento di Chimica, Sapienza University, P. le Aldo Moro 5, Roma, Italy*

(Received 17 April 2018; accepted 23 May 2018; published online 7 June 2018)

One of the outstanding features of ionic liquids is their inherently hierarchical structural organization at mesoscopic spatial scales. Recently experimental and computational studies showed the fading of this feature when pressurising. Here we use simulations to show that this effect is not general: appropriate anion choice leads to an obstinate resistance against pressurization. *Published by AIP Publishing.* <https://doi.org/10.1063/1.5036588>

Room Temperature Ionic Liquids (RTILs) are ionic compounds with a melting point below ambient temperature. They are characterised by a range of appealing properties including a large liquid state window, enhanced thermal and electrochemical stability, and a wide tunability of chemo-physical properties upon little changes in their chemical architecture.^{1–5} Their mesoscopic order is under constant exploration, after simulations and experimental studies highlighted the existence of a highly hierarchical morphology over a spatial scale encompassing from Angstrom up to several nm's. As a matter of fact, their structure that was originally considered to be characterised by an onion-like alternation of opposite sign ions (similarly to the organisation in conventional high temperature molten salt, e.g., NaCl) has been discovered to show an enhanced level of organization, stemming from the alternation not only of charged and uncharged moieties, but also of polar and apolar domains.^{6–21} These alternations are now known to be fingerprinted by well-defined X-ray and/or neutron scattering^{13,21–24} features in the low momentum transfer (Q) range. The interest toward this feature is witnessed by the wealth of studies addressing its nature and dependence upon chemical nature of the ions,^{25–30} temperature,^{13,15,31} mixture composition,^{32–41} and, only recently, pressure.^{42–45}

High pressure studies are an important tool to explore the details of microscopic and mesoscopic correlations in complex materials. Pressure changes allow investigating intermolecular interactions, by inducing density changes without introducing the chaotic perturbation that temperature changes induce. As a matter of fact, while temperature dependence studies of morphology in RTILs have been reported in the past,^{13,15,31} the pressure dependence of the mesoscopic organization in aprotic RTILs has been explored by means of experimental X-ray studies^{42–44} and simulations^{45–50} only in the last couple of years. Confirming a trend that has been progressing in the field of RTILs over the last decades, the

synergic use of scattering (as well as other spectroscopic) experiments and Molecular Dynamics (MD) simulations has provided a great deal of understanding on the nature of mesoscopic organization in RTILs under pressure. The first experimental study by Yoshimura *et al.* reported the Small Angle X-ray Scattering (SAXS) patterns from a series of 1-alkyl,3-methylimidazolium tetrafluoroborate (hereinafter indicated as [C_nmim][BF₄]) at ambient temperature and pressure as high as 3.9 GPa.⁴² Therein the progressive position shift and amplitude vanishing of the low Q peak centred at ca. 3 nm⁻¹ had been observed. Such a behavior has been rationalised by some of us by means of MD simulations⁴⁵ that accounted in an essentially quantitative way for the peak shift and fading upon pressure increase: the proposed mechanism for such a phenomenology is related to the progressive curling of the side alkyl chain from a quite stretched conformation at ambient conditions to a kinked one when pressure increases. Such a profound deformation of the alkyl side chain arrangement leads to the progressive dissolving of the polar-apolar alternation that is fingerprinted by the low Q peak. While the polar, charged part of the system is barely affected by pressure, the apolar moieties are strongly deformed by the application of pressure. Following this report, a related simulation study described the evolution of mesoscopic order in 1-alkyl-1-methylpyrrolidinium bis(trifluoromethylsulfonyl) amide ([pyrr_{1x}][Tf₂N], with x = 8 and 10) with pressure and similar results have been observed, with the low Q peak related to polar-apolar alternation disappearing upon the application of pressure.⁴⁶ The overall description of the effect of pressure on mesoscopic order in RTILs seems then to be quite clear and straightforward. Recently, however, some new studies appeared that prompt for further investigation. Following the mentioned papers, Dhungana and Margulis described the role of pressure on affecting the mesoscopic order in imidazolium-based RTILs with alkyl or ether side-chains.⁴⁸ The latter kind of RTILs is well known to be characterised by X-ray diffraction patterns that do not show a low Q peak^{14,15,51–54} due to the enhanced polarity of ether-containing side chains that lead to a vanishing polar-apolar alternation. In the mentioned study, the authors found that an increase in pressure from 0.1 MPa to 1.2 GPa leads to a

^{a)}Author to whom correspondence should be addressed: olga.russina@uniroma1.it

substantial decrease of the low Q peak amplitude in 1-decyl,3-methylimidazolium bis(trifluoromethylsulfonyl)amide (hereinafter indicated as $[\text{C}_{10}\text{mim}][\text{Tf}_2\text{N}]$). They rationalised this observation in terms of a deformation of the side alkyl chain conformation similar to what was observed in Ref. 45, observing that while at ambient conditions the chains point radially toward the centre of the apolar domains, in the high pressure regime, tails curl, tending to lay flat or parallel to the interface between neutral and charged domains. Recently however Yoshimura and co-workers reported a joint high pressure Raman and SAXS study of $[\text{C}_n\text{mim}][\text{Tf}_2\text{N}]$ with $3 \leq n \leq 10$, where they showed that, at odd with the case of $[\text{C}_n\text{mim}][\text{BF}_4]$ (where the low Q peak vanishes with pressure), $[\text{C}_n\text{mim}][\text{Tf}_2\text{N}]$ RTILs are characterised by an essentially not vanishing low Q peak up to the upper pressure that they explored, i.e., 2.5 GPa.⁴⁴ This finding has to be related to another experimental study by Pilar and co-workers, who investigated the effect of pressure on the mesoscopic organization in a series of N -alkyl- N -methyl-pyrrolidinium bis(trifluoromethanesulfonyl)imide RTILs ($[\text{pyrr}_{1x}][\text{Tf}_2\text{N}]$, with $x = 3, 6, \text{ and } 9$), as well as their mixtures with LiTf_2N .⁴³ They show SAXS data on $[\text{pyrr}_{19}][\text{Tf}_2\text{N}]$, where the low Q peak maintains an appreciable amplitude even up to 8.7 GPa. This experimental observation is at odd with MD simulations on related RTILs by Sharma *et al.*⁴⁶ The puzzling resilience of mesoscopic structure in $[\text{Tf}_2\text{N}]$ -based RTILs toward pressure application prompted us to explore this behavior in more detail. Accordingly we developed a series of molecular dynamics simulations of $[\text{C}_8\text{mim}][\text{Tf}_2\text{N}]$ at 303 K and different values of pressure, ranging between ambient and 2.5 GPa. While computational details are provided in the [supplementary material](#), herein we mention that we used cubic simulation boxes with large enough sides to allow for an accurate determination of the mesoscopically segregated nature of the morphology in this compound. Moreover, especially at the highest pressures that were investigated, special care was taken in verifying that the system reached equilibrium without appreciable changes in structure when prolonging the simulation (see Fig. S1 of the [supplementary material](#)). We also stress that we used the force field developed by Köddermann *et al.*⁵⁵ to account for interactions. Such a choice is different from the one made in previous related studies^{46,48} and is justified by the excellent agreement of computed density, viscosity, and self-diffusion coefficient that this parametrization provides.⁵⁵ The present MD simulation of $[\text{C}_8\text{mim}][\text{Tf}_2\text{N}]$ at ambient conditions adequately accounts for the X-ray diffraction pattern that some of

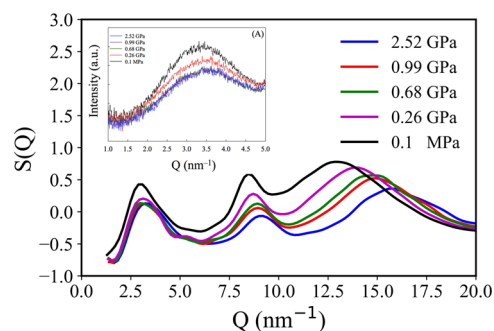


FIG. 1. Pressure dependence (from ambient to 2.5 GPa) of the computed X-ray diffraction pattern for $[\text{C}_8\text{mim}][\text{Tf}_2\text{N}]$ at 303 K. In the inset, the experimental SAXS data sets published by Yoshimura *et al.*⁴⁴ on the same RTIL at 298 K as a function of pressure are shown. [Reproduced with permission from Yoshimura *et al.*, Phys. Chem. Chem. Phys. **20**, 199 (2018). Copyright 2018 PCCP Owner Societies.]

us published in the past⁵⁶ (see Fig. S2 of the [supplementary material](#)), in agreement with more recent results from other groups.⁵⁷

Figure 1 shows then the pressure dependence (from ambient pressure to 2.5 GPa) of a portion ($Q < 20 \text{ nm}^{-1}$) of the computed X-ray diffraction pattern; in the inset, the published data by Yoshimura *et al.* for the same RTIL are shown [note that these data sets cover a more limited Q range ($Q < 5 \text{ nm}^{-1}$)].⁴⁴ The computed patterns show three diffraction features centred at approximately $Q_1 = 3.5$, $Q_2 = 8$, and $Q_3 = 13 \text{ nm}^{-1}$: they have been related to polarity, charge, and adjacency alternations, respectively.¹⁷⁻¹⁹ It is noteworthy that, similarly to the experimental data, the peak centred at Q_1 slightly decreases its amplitude when passing from ambient to 0.68 GPa but then maintains essentially unaltered upon further pressurization (we also stress the fact that experimental patterns do not show indication of the appearing of Bragg peaks that might indicate an amorphous-crystalline phase transition over the probed pressure range). Our simulated data are also qualitatively consistent with the recently reported X-ray scattering data on amorphous $[\text{C}_2\text{mim}][\text{Tf}_2\text{N}]$ at ambient pressure and 3.4 GPa at room temperature, considering that the latter RTIL bears a short ethyl chain that leads to no peak at Q_1 .⁵⁸ The trend shown in figure then provides indication of a strong resistance of the mesoscopic organization in $[\text{C}_8\text{mim}][\text{Tf}_2\text{N}]$ against external pressure, in agreement with the observation made by Yoshimura *et al.*,⁴⁴ at odd with the behavior shown by $[\text{C}_8\text{mim}][\text{BF}_4]$. The peak centred at Q_1 also shows a very limited shift in position upon pressurization, in agreement

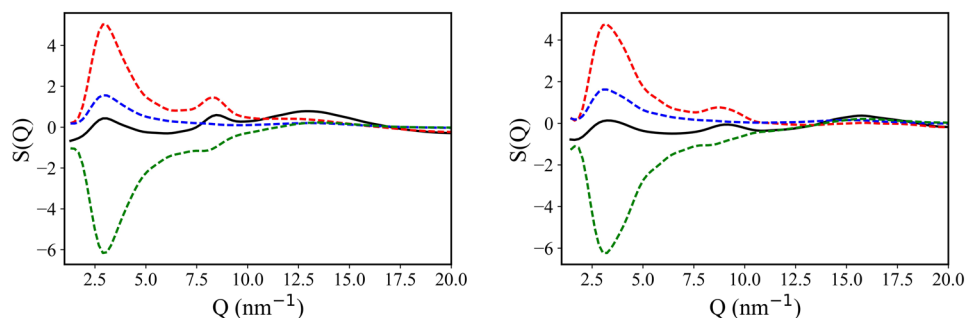


FIG. 2. Pressure dependence [ambient condition (left) and 2.5 GPa (right)] of the computed X-ray diffraction pattern for $[\text{C}_8\text{mim}][\text{Tf}_2\text{N}]$ at 303 K (black) and its decomposition into polar-polar (red), apolar-apolar (blue), and polar-apolar (green) components.

with experimental results.⁴⁴ A decomposition of the computed diffraction patterns at ambient pressure and at 2.5 GPa in terms of the polar-polar, apolar-apolar, and polar-apolar contributions (see Fig. 2), as proposed originally by Margulis *et al.*,^{17–19} indicates that even up to pressures of the order of 2.5 GPa, the characteristic polar-apolar alternation that characterises the RTILs' morphology at ambient conditions is maintained essentially unaffected: the observed low Q peak centred at Q_1 fingerprints the existence of alternating polar and polar domains and this structural organization at mesoscopic scales is hardly affected by pressures as high as 2.5 GPa. In Fig. S4 of the [supplementary material](#), we show the pressure dependence of polar/apolar contributions to the computed X-ray and neutron scattering patterns for both $[\text{C}_8\text{mim}][\text{Tf2N}]$ and $[\text{C}_8\text{mim}][\text{BF}_4]$, highlighting the substantially different high pressure response of these two RTILs. Furthermore we note that a distinct pressure dependence of peaks Q_2 (mildly shifting to high Q) and Q_3 (strongly shifting to high Q) can be observed. While no experimental information exists on such a trend for $[\text{C}_8\text{mim}][\text{Tf2N}]$, Pilar *et al.*'s paper on $[\text{pyrr}_{19}][\text{Tf2N}]$ shows a similar behavior for both peaks at Q_2 and Q_3 that shift toward higher Q values, upon pressurization.⁴³

Figure 3 shows the pressure dependence of the intramolecular distance distribution function (ddf) between the ring nitrogen atom bearing the octyl chain and the terminal carbon of the octyl chain. A decrease of the amplitude of the large distance peaks can be observed, witnessing a progressive curling of the octyl chain; however, the change is not as large as the one observed by us for the case of $[\text{C}_8\text{mim}][\text{BF}_4]$. In the [supplementary material](#), we report a comparison between these ddf's for $[\text{C}_8\text{mim}][\text{Tf2N}]$ and $[\text{C}_8\text{mim}][\text{BF}_4]$, at ambient pressure and 1 GPa (Fig. S5 of the [supplementary material](#)). It appears that the presence of the $[\text{Tf2N}]$ anion confers a larger resistance toward tail curling upon pressurizing. This behavior has been further explored using spatial distribution functions (sdf's) describing how the anion and the terminal intramolecular CH_3 group distribute around a central reference cation.

Figure 4 shows such sdf's for $[\text{C}_8\text{mim}][\text{BF}_4]$ ⁴⁵ and $[\text{C}_8\text{mim}][\text{Tf2N}]$ at ambient pressure and at 1 GPa.

The $[\text{BF}_4]$ anion coordination around the imidazolium ring is not influenced by the increasing pressure, and it is organised in such a way that, upon pressurization, the curled side

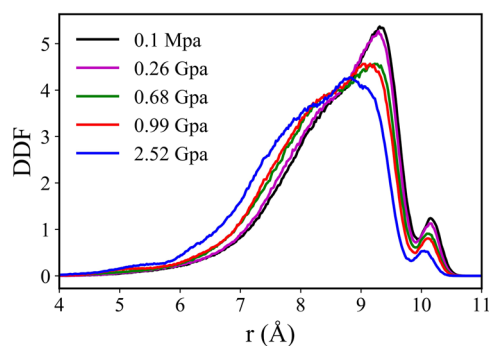


FIG. 3. Distance distribution function (ddf) for the ring nitrogen atom bearing the octyl chain and the terminal carbon of the octyl chain, as extracted from MD simulations of $[\text{C}_8\text{mim}][\text{Tf2N}]$ at 303 K at different pressures, between ambient and 2.5 GPa.

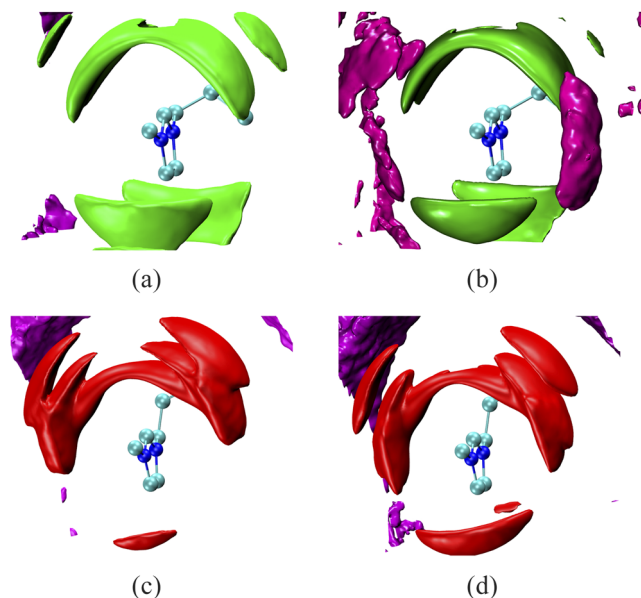


FIG. 4. Spatial distribution functions describing the distribution of the $[\text{BF}_4]$ anion (green), $[\text{Tf2N}]$ anion (red), and terminal methyl group (magenta) from molecular dynamics simulations of $[\text{C}_8\text{mim}][\text{BF}_4]$ (data taken from Ref. 45) [panels (a) and (b)] and $[\text{C}_8\text{mim}][\text{Tf2N}]$ [panels (c) and (d)], at ambient pressure [panels (a) and (c)] and 1 GPa [panels (b) and (d)]. Isovalues are taken at 30% of their maximum value. The magenta spot close to the imidazolium ring in $[\text{C}_8\text{mim}][\text{BF}_4]$ at high pressure (panel b) fingerprints the octyl chain curling upon pressurization and has no counterpart in the case of $[\text{C}_8\text{mim}][\text{Tf2N}]$ (panel d). [Adapted with permission from Russina *et al.*, Phys. Chem. Chem. Phys. **17**, 29496 (2015). Copyright 2015 PCCP Owner Societies.]

chain has accessible space to locate below and above the imidazolium ring (as witnessed by the magenta lobes developing therein only at high pressure [Fig. 4(b)]; on the other hand, the $[\text{Tf2N}]$ anion distribution around the cation hinders the access of the side chain to those locations and, at odd with the $[\text{C}_8\text{mim}][\text{BF}_4]$ case, no magenta lobes develop at high pressure [see Fig. 4(d)]. Such a behavior is consistent with the crystal structures of related compounds such as $[\text{C}_2\text{mim}][\text{BF}_4]$ ⁵⁹ and $[\text{C}_2\text{mim}][\text{Tf2N}]$.⁶⁰ Selected snapshots extracted from the crystal structures published therein are reported in Fig. S6 of the [supplementary material](#). There one can appreciate that in their crystal states, $[\text{BF}_4]$ anions tend to occupy bridging positions between two stacked imidazolium rings: accordingly, upon pressure application, the interlayer between two rings is empty and the octyl chains can easily occupy that space, once folding, leading to the trend depicted in Figs. 4(a) and 4(b). On the other hand, $[\text{Tf2N}]$ anions tend to occupy the space between two stacked imidazolium rings: in order for the octyl chains to occupy to those locations, they must first shift the anions that are located therein. Such a situation then strongly disfavours the curling of the octyl tails. Recent MD simulations conducted on $[\text{C}_n\text{mim}][\text{X}]$, with $[\text{X}]$ being different anions, showed that also in the liquid state, the $[\text{Tf2N}]$ anion, due to its bulkiness, tends to lay above and below the imidazolium ring, while the $[\text{BF}_4]$ anion prefers being localised equatorially with respect to the imidazolium ring, in the neighbourhood of the hydrogen atoms.^{61,62} These computational observations agree with the mechanism that we are presently indicating to rationalise the experimental evidence.

At the present stage, we propose that the different experimental behavior observed for the pressure response of the

mesoscopic organization in RTILs bearing either [BF₄] or [Tf₂N] anions might be related to the different stable location for the anions with respect to the local packing of neighbour cations. The presence of sandwiched [Tf₂N] anions between neighbour imidazolium rings leads to a strong hindrance for the side chains to curl and consequently dissolve the polar-apolar alternation at high pressure; on the other hand, the preferred location of [BF₄] anions favours the mentioned curling and the consequent change in structural organization. Once again, we believe that RTILs show a wealth of complex behaviors that confirm the term designer solvent^{4,5} used for these compounds to indicate the large opportunities to fine tune their behavior upon small chemical changes.

See [supplementary material](#) for further computational details and additional figures.

This work has been supported by the University of Rome Sapienza Project: “Microscopic and mesoscopic organization in ionic liquid-based systems” (No. RG11715C7CC660BE).

We wish to dedicate this contribution to the memory of the late Professor K. R. Seddon.

- ¹M. J. Earle and K. R. S. Seddon, *Pure Appl. Chem.* **72**, 1391 (2000).
²K. R. S. Seddon, *J. Chem. Technol. Biotechnol.* **68**, 351 (1997).
³R. D. Rogers and K. R. S. Seddon, *Science* **302**, 792 (2003).
⁴N. V. Plechkova and K. R. Seddon, in *Methods and Reagents for Green Chemistry: An Introduction*, edited by P. Tundo, A. Perosa, and F. Zecchini (John Wiley & Sons, Inc., Hoboken, NJ, USA, 2007), pp. 103–130.
⁵M. Freemantle, *Chem. Eng. News* **76**, 32 (1998).
⁶S. M. Urahata and M. C. C. Ribeiro, *J. Chem. Phys.* **120**, 1855 (2004).
⁷M. G. Del Pópolo and G. A. Voth, *J. Phys. Chem. B* **108**, 1744 (2004).
⁸Y. Wang and G. A. Voth, *J. Phys. Chem. B* **110**, 18601 (2006).
⁹Y. Wang and G. A. Voth, *J. Am. Chem. Soc.* **127**, 12192 (2005).
¹⁰J. N. Canongia Lopes and A. A. H. Pádua, *J. Phys. Chem. B* **110**, 3330 (2006).
¹¹A. A. H. Pádua, M. F. Costa Gomes, and J. N. Canongia Lopes, *Acc. Chem. Res.* **40**, 1087 (2007).
¹²J. N. Canongia Lopes, M. F. Costa Gomes, and A. A. H. Pádua, *J. Phys. Chem. B* **110**, 16816 (2006).
¹³A. Triolo, O. Russina, H.-J. Bleif, and E. Di Cola, *J. Phys. Chem. B* **111**, 4641 (2007).
¹⁴O. Russina and A. Triolo, *Faraday Discuss.* **154**, 97 (2012).
¹⁵O. Russina, A. Triolo, L. Gontrani, and R. Caminiti, *J. Phys. Chem. Lett.* **3**, 27 (2012).
¹⁶O. Russina, F. Lo Celso, N. V. Plechkova, and A. Triolo, *J. Phys. Chem. Lett.* **8**, 1197 (2017).
¹⁷H. V. R. Annapureddy, H. K. Kashyap, P. M. De Biase, and C. J. Margulis, *J. Phys. Chem. B* **114**, 16838 (2010).
¹⁸H. K. Kashyap, J. J. Hettige, H. V. R. Annapureddy, and C. J. Margulis, *Chem. Commun.* **48**, 5103 (2012).
¹⁹J. C. Araque, J. J. Hettige, and C. J. Margulis, *J. Phys. Chem. B* **119**, 12727 (2015).
²⁰H. K. Kashyap, C. S. Santos, N. S. Murthy, J. J. Hettige, K. Kerr, S. Ramati, J. Gwon, M. Gohdo, S. I. Lall-Ramnarine, J. F. Wishart, C. J. Margulis, and E. W. Castner, *J. Phys. Chem. B* **117**, 15328 (2013).
²¹R. Hayes, G. G. Warr, and R. Atkin, *Chem. Rev.* **115**, 6357 (2015).
²²K. Fujii, R. Kanzaki, T. Takamuku, Y. Kameda, S. Kohara, M. Kanakubo, M. Shibayama, S. Ishiguro, and Y. Umeyayashi, *J. Chem. Phys.* **135**, 244502 (2011).
²³R. Atkin and G. G. Warr, *J. Phys. Chem. B* **112**, 4164 (2008).
²⁴R. Hayes, S. Imberti, G. G. Warr, and R. Atkin, *Phys. Chem. Chem. Phys.* **13**, 3237 (2011).
²⁵L. Gontrani, O. Russina, F. Lo Celso, R. Caminiti, G. Annat, and A. Triolo, *J. Phys. Chem. B* **113**, 9235 (2009).
²⁶S. Li, J. L. Banuelos, J. Guo, L. Anovitz, G. Rother, R. W. Shaw, P. C. Hillesheim, S. Dai, G. A. Baker, and P. T. Cummings, *J. Phys. Chem. Lett.* **3**, 125 (2012).
²⁷C. S. Santos, N. S. Murthy, G. A. Baker, and E. W. Castner, *J. Chem. Phys.* **134**, 121101 (2011).
²⁸A. Triolo, O. Russina, B. Fazio, G. B. Appetecchi, M. Carewska, and S. Passerini, *J. Chem. Phys.* **130**, 164521 (2009).
²⁹O. Russina, L. Gontrani, B. Fazio, D. Lombardo, A. Triolo, and R. Caminiti, *Chem. Phys. Lett.* **493**, 259 (2010).
³⁰M. Mizuhata, T. Minowa, and S. Deki, *Electrochemistry* **77**, 725 (2009).
³¹B. Aoun, M. A. González, M. Russina, D. L. Price, and M.-L. Saboungi, *J. Phys. Soc. Jpn.* **82**, SA002 (2013).
³²M. Liang, S. Khatun, and E. W. Castner, *J. Chem. Phys.* **142**, 121101 (2015).
³³O. Russina, A. Sferrazza, R. Caminiti, and A. Triolo, *J. Phys. Chem. Lett.* **5**, 1738 (2014).
³⁴T. Murphy, R. Hayes, S. Imberti, G. G. Warr, and R. Atkin, *Phys. Chem. Chem. Phys.* **16**, 13182 (2014).
³⁵R. Hayes, S. Imberti, G. G. Warr, and R. Atkin, *Angew. Chem., Int. Ed. Engl.* **51**, 7468 (2012).
³⁶H. J. Jiang, P. A. Fitzgerald, A. Dolan, R. Atkin, and G. G. Warr, *J. Phys. Chem. B* **118**, 9983 (2014).
³⁷L. M. Varela, T. Méndez-Morales, J. Carrete, V. Gómez-González, B. Docampo-Álvarez, L. J. Gallego, O. Cabeza, and O. Russina, *J. Mol. Liq.* **210**, 178 (2015).
³⁸O. Russina, M. Macchiagodena, B. Kirchner, A. Mariani, B. Aoun, M. Russina, R. Caminiti, and A. Triolo, *J. Non-Cryst. Solids* **407**, 333 (2015).
³⁹W. Schroer, A. Triolo, and O. Russina, *J. Phys. Chem. B* **120**, 2638 (2016).
⁴⁰O. Russina, R. Caminiti, T. Méndez-Morales, J. Carrete, O. Cabeza, L. J. Gallego, L. M. Varela, and A. Triolo, *J. Mol. Liq.* **205**, 16 (2015).
⁴¹H. Montes-Campos, J. M. Otero-Mato, T. Méndez-Morales, E. López-Lago, O. Russina, O. Cabeza, L. J. Gallego, and L. M. Varela, *J. Chem. Phys.* **146**, 124503 (2017).
⁴²Y. Yoshimura, M. Shigemi, M. Takaku, M. Yamamura, T. Takekiyo, H. Abe, N. Hamaya, D. Wakabayashi, K. Nishida, N. Funamori, T. Sato, and T. Kikegawa, *J. Phys. Chem. B* **119**, 8146 (2015).
⁴³K. Pilar, V. Balédent, M. Zeghal, P. Judeinstein, S. Jeong, S. Passerini, and S. Greenbaum, *J. Chem. Phys.* **148**, 031102 (2018).
⁴⁴Y. Yoshimura, T. Takekiyo, Y. Koyama, M. Takaku, M. Yamamura, N. Kikuchi, D. Wakabayashi, N. Funamori, K. Matsuishi, H. Abe, and N. Hamaya, *Phys. Chem. Chem. Phys.* **20**, 199 (2018).
⁴⁵O. Russina, F. Lo Celso, and A. Triolo, *Phys. Chem. Chem. Phys.* **17**, 29496 (2015).
⁴⁶S. Sharma, A. Gupta, and H. K. Kashyap, *J. Phys. Chem. B* **120**, 3206 (2016).
⁴⁷S. Sharma, A. Gupta, D. Dhabal, and H. K. Kashyap, *J. Chem. Phys.* **145**, 134506 (2016).
⁴⁸K. B. Dhungana and C. J. Margulis, *J. Phys. Chem. B* **121**, 6890 (2017).
⁴⁹Y. Zhao, X. Liu, X. Lu, S. Zhang, J. Wang, H. Wang, G. Gurau, R. D. Rogers, L. Su, and H. Li, *J. Phys. Chem. B* **116**, 10876 (2012).
⁵⁰J. K. Shah and E. J. Maginn, *Fluid Phase Equilib.* **294**, 197 (2010).
⁵¹A. Triolo, O. Russina, R. Caminiti, H. Shirota, H. Y. Lee, C. S. Santos, N. S. Murthy, and E. W. Castner, *Chem. Commun.* **48**, 4959 (2012).
⁵²K. Shimizu, C. E. S. Bernardes, A. Triolo, and J. N. Canongia Lopes, *Phys. Chem. Chem. Phys.* **15**, 16256 (2013).
⁵³H. K. Kashyap, C. S. Santos, R. P. Daly, J. J. Hettige, N. S. Murthy, H. Shirota, E. W. Castner, and C. J. Margulis, *J. Phys. Chem. B* **117**, 1130 (2013).
⁵⁴J. J. Hettige, W. D. Amith, E. W. Castner, and C. J. Margulis, *J. Phys. Chem. B* **121**, 174 (2017).
⁵⁵T. Köddermann, D. Paschek, and R. Ludwig, *Chem. Phys. Chem* **8**, 2464 (2007).
⁵⁶E. Bodo, L. Gontrani, R. Caminiti, N. V. Plechkova, K. R. S. Seddon, and A. Triolo, *J. Phys. Chem. B* **114**, 16398 (2010).
⁵⁷K. Fujii, S. Kohara, and Y. Umeyayashi, *Phys. Chem. Chem. Phys.* **17**, 17838 (2015).
⁵⁸L. F. O. Faria, T. A. Lima, and M. C. C. Ribeiro, *Cryst. Growth Des.* **17**, 5384 (2017).
⁵⁹A. R. Choudhury, N. Winterton, A. Steiner, A. I. Cooper, and K. A. Johnson, *J. Am. Chem. Soc.* **127**, 16792 (2005).
⁶⁰A. R. Choudhury, N. Winterton, A. Steiner, A. I. Cooper, and K. A. Johnson, *CrystEngComm* **8**, 742 (2006).
⁶¹G.-E. Logotheti, J. Ramos, and I. G. Economou, *J. Phys. Chem. B* **113**, 7211 (2009).
⁶²K. R. Ramya, P. Kumar, and A. Venkatnathan, *J. Phys. Chem. B* **119**, 14800 (2015).